

# Electronic Transport through $\text{YBa}_2\text{Cu}_3\text{O}_{7-x}$ Grain Boundary Interfaces between 4.2 K and 300 K

C. W. Schneider, S. Hembacher, G. Hammerl, R. Held, A. Schmehl, A. Weber,  
T. Kopp, and J. Mannhart

Experimentalphysik VI, Center for Electronic Correlations and Magnetism, Institute of Physics,  
Augsburg University, D-86135 Augsburg, Germany

(April 14, 2024)

## Abstract

The current-induced dissipation in  $\text{YBa}_2\text{Cu}_3\text{O}_{7-x}$  grain boundary tunnel junctions has been measured between 4.2 K and 300 K. It is found that the resistance of 45 (100)/(110) junctions decreases linearly by a factor of four when their temperature is increased from 100 K to 300 K. At the superconducting transition temperature  $T_c$  the grain boundary resistance of the normal state and of the superconducting state extrapolate to the same value.

74.20.Rp, 74.50.+r, 74.76.Bz, 85.25.Cp

Soon after the discovery of superconductivity in  $\text{La}_{2-x}\text{Ba}_x\text{CuO}_4$  [1] it was realized that the normal-state properties of the high- $T_c$  cuprates differ significantly from those of the low- $T_c$  superconductors. The most prominent and still unexplained normal state properties of the high- $T_c$  compounds are the linear temperature dependence of the in-plane resistivity in the optimally doped compounds [2], spin and charge inhomogeneities [3], and the pseudogap present in the underdoped regime [4].

The complex electronic behavior of the high- $T_c$  materials is also reflected in the characteristics of their interfaces. For  $T < T_c$ , for example, large-angle grain boundaries are excellent tunnelling barriers [5], a feature unknown from conventional superconductors. Several mechanisms responsible for the electronic transport properties of grain boundaries and other interfaces have been identified for the temperature range below  $T_c$ , such as the  $d_{x^2-y^2}$  dominated order parameter symmetry, structural effects and space charge layers [5]. In fact, grain boundaries operated below  $T_c$  have been used to reveal fundamental properties of the high- $T_c$  cuprates, such as the existence of Cooper pairs [6] or the unconventional order parameter symmetry [7].

As is the case for  $T < T_c$ , we expect valuable information on the interfaces of the cuprates, or even on the bulk materials themselves, to be contained in the tunneling characteristics of grain boundaries for  $T > T_c$ . However, only very few data are available for this temperature regime [5,8]. This lack of data arises from the difficulty to measure the grain boundary current-voltage ( $I(V_{gb})$ ) characteristics free of voltages produced by the bridges that are needed to contact the interfaces. By utilizing a difference-technique to subtract these unwanted voltages, we have now succeeded in measuring the current-voltage characteristics of  $\text{YBa}_2\text{Cu}_3\text{O}_{7-\delta}$  grain boundaries for  $4.2\text{ K} < T < 300\text{ K}$ . These studies provide evidence that the normal state resistance of  $45^\circ(100)/(110)$  tilt grain boundaries is not influenced by the onset of the superconducting transition. The experiments furthermore reveal that for  $T > T_c$  the resistance of these grain boundaries decreases linearly with increasing temperature.

The experiments were performed with bicrystalline  $\text{YBa}_2\text{Cu}_3\text{O}_{7-\delta}$  films grown by pulsed laser deposition at  $760^\circ\text{C}$  in  $0.25\text{ mbar}$  of  $\text{O}_2$  to a typical thickness of  $40\{50\text{ nm}$ . The  $\text{SrTiO}_3$ -

substrates contained symmetric and (100)/(110)-asymmetric 45° [001]-tilt grain boundaries, specified to within 1°. After deposition, the samples were cooled during two hours in an  $O_2$ -pressure of 400 mbar. Because the deposition geometry was tuned to optimize the homogeneity of the samples,  $T_c$  varied by less than 0.5 K across the wafers, while the thickness variations were smaller than 10%. For the four-point measurements, gold contacts were structured photolithographically before the  $YBa_2Cu_3O_{7-x}$  films were patterned by etching in a  $H_3PO_4$  solution, or by dry etching with an Ar ion-beam. The  $YBa_2Cu_3O_{7-x}$  bridges had widths and lengths between the voltage probes of 2.5  $\mu m$  and 30  $\mu m$ , respectively (see Fig. 1), and their  $T_c$  varied less than 200 mK. In addition, several samples were patterned into Wheatstone-bridge configurations, of which each arm consists of a meander line containing 23 straight sections with widths of 6  $\mu m$ . Two of the meander lines were patterned such that each of the 23 sections crosses the boundary once.

The technique to measure precisely the grain boundary resistance  $R_{gb}$  below  $T_c$  is based on measuring the  $I(V_{gb})$  characteristics of the Josephson junctions while applying a microwave field large enough to suppress their critical current. For this purpose, we used low frequency microwaves ( $< 10$  GHz) to avoid inaccuracies resulting from the Shapiro steps.

All measurements were conducted in shielded rooms using motor-driven dip-sticks. The samples were cooled at 4.2 K in liquid Helium, at 77 K in liquid nitrogen, and at other temperatures via He or  $N_2$  vapor and thermal conduction across the sample holder. Immersion into the cooling liquids did not affect the characteristics, providing evidence that selfheating is insignificant under the experimental conditions.

For  $T > T_c$  the transport properties of the interfaces cannot be measured with a straightforward four-point technique because the voltage  $V_{meas}$  generated by a bridge straddling the boundary is composed of two contributions: a) the grain boundary voltage  $V_{gb}$  and b) the voltages  $V_{g1}$  and  $V_{g2}$  caused by the resistive grains inside the bridge. This problem can be solved by subtracting from  $V_{meas}$  the grain contributions  $V_{g1}$  and  $V_{g2}$ . For this,  $V_{g1}$  and  $V_{g2}$  are obtained by approximating them with the voltages  $V_{g1}^?$  and  $V_{g2}^?$  generated by independent intragrain bridges that are measured simultaneously. Not surprisingly, test measurements

revealed variations of  $V_{g1}^?$  and  $V_{g2}^?$  of several percent as a function of the bridge location. Therefore, the intragrain bridges were placed as closely as possible to the boundary bridge (see Fig. 1). The desired measurement accuracy also determined the optimum size of the bridges. On the one hand the bridges were patterned to be as small as possible so that they could be located close to the grain boundary. On the other hand, their size was chosen to be large enough for the patterning-induced scatter of the bridge aspect ratios to be insignificant. In samples optimized this way, the voltages across the two bridges  $V_{g1}^?$  and  $V_{g2}^?$  were identical to within 1% at 100 K and to 0.3% for  $T > 200$  K. Therefore the grain boundary voltage equals with the same accuracy  $V_{gb} = V_{meas} - (V_{g1}^? + V_{g2}^?) = 2$ .

As introduced by Mathur et al. [9] for studies of  $\text{La}_{1-x}\text{Ca}_x\text{MnO}_3$  bicrystals, and similar to the work described in Ref. [8], we also patterned several samples into Wheatstone-bridges. This approach has the advantage that the generated voltages are huge and that  $V_{g1}^?$  and  $V_{g2}^?$  are subtracted from  $V_{meas}$  already during the measurement. Having performed measurements with such bridges, we checked their balance by photolithographically cutting the Wheatstone-configurations, to individually assess the resistances of the meander lines. Because these studies revealed  $T$  dependent balancing errors of 1-10%, we preferred the three-bridge approach for measurements of the  $R_{gb}(T)$  characteristics, while Wheatstone-bridges were chosen when a large signal was required, as was the case for some studies of  $I(V)$  characteristics.

To gain insight into the electronic transport mechanisms, we measured the  $I(V)$  characteristics between 4.2 K and 300 K by using Wheatstone-bridges. For  $T > T_c$  the characteristics are non-linear on this large voltage scale, in particular below 150 K (see Fig. 2). Analyzing the non-linearity, we first note that the microstructure of the grain boundaries is inhomogeneous down to the unit cell level [5]. The  $I(V)$  curves are therefore generated by large numbers of microstructurally different channels connected in parallel. The behavior of the averaged junctions is consistent with the one of a back-to-back Schottky contact as predicted by the band bending model [10]. If tentatively described by a Simmons-t [11], the averaged  $I(V)$  characteristics correspond to heights and widths of hypothetical effective

junction barriers of  $\sim 100$  meV and  $\sim 1.2$  nm. Thus, these data suggest unusually small barrier heights. They are, in particular, much smaller than the energy scale of grain boundary built-in potentials measured by electron-holography of  $\sim 2$  eV [12].

At small voltages,  $V_{gb} < 10$  mV, the non-linearity of the  $I(V)$  curves is insignificant, and they are characterized by their ohmic resistance, which can be obtained by selecting an appropriate voltage ( $V_{cr}$ ) or current ( $I_{cr}$ ) criterion  $V_{cr} = I_{cr} R_{gb} < 10$  mV. For  $T < T_c$ , due to the microwave irradiation, the  $I(V)$  characteristics are linear, too, even over a larger voltage range. The only exception is given by 45 boundaries at  $T < 40$  K, which will be discussed below. Applying the three-bridge technique, we were therefore able to deduce the  $R_{gb}(T)$  dependence of a given grain boundary by measuring in one temperature sweep from 4.2 K to 300 K just one boundary bridge plus the two intragrain reference bridges. Hereby one voltage or current criterion, typically  $I_{cr} = 100$  A, is used for all temperatures.

The  $R(T)$ -dependence of a 45  $\mu$ m symmetric grain boundary measured this way is presented in Fig. 3. The resistance-area product  $R_{gb}A(77\text{ K}) \sim 1 \cdot 10^{-8}$  cm<sup>2</sup> compares well with literature values [5]. Three remarkable features are displayed by the temperature dependence of the resistance. First, the resistance reaches a maximum at  $\sim 30$  K (see also Fig. 4). This maximum is not displayed by symmetric 24 and 36 boundaries measured as reference samples. Second, around  $T_c$  the resistance develops a distinct peak structure. This peak, which is not associated with the microwave irradiation, was found to vary from sample to sample, and to change with time over weeks. Except for this peak, the grain boundary resistance of the normal state and of the superconducting state extrapolate within the measurement accuracy of  $\sim 2\%$  to the same value  $R_{gb}(T_c) = 10.7$  . This temperature dependence is characteristic for all samples we have studied, except for few that displayed at  $T_c$  a resistance step of  $< 5\%$  . As this step was found to be not reproducible and to increase for a given sample over weeks, we consider it to be an artifact resulting from chemical reactions or diffusion. Third, between 100 K and 300 K the resistance decreases with increasing temperature by a factor of four. The temperature dependence is hereby remarkably linear, with a barely noticeable positive curvature (Fig. 3, upper inset). This is in striking contrast to

the linear resistance increase of the adjacent  $\text{YBa}_2\text{Cu}_3\text{O}_{7-x}$  grains (Fig. 3, lower inset). In the following, we will discuss the three features and their implications for the understanding of the interfaces, beginning with the superconducting regime.

At low temperatures, the resistance of 45° grain boundaries changes non-monotonically with  $T$ , and even depends on the value of the tunneling current (see Fig. 4). This maximum and its current bias dependence are consistent with the formation of a zero-bias anomaly by the faceted 45° junctions. At small bias currents  $V_{gb}$  is of the order 1 mV, and therefore sufficiently small to probe the temperature dependent shape of the zero-bias conductance peak in the superconducting energy gap. This zero-bias conductance peak is usually presumed to arise from Andreev bound states generated by the  $d_{x^2-y^2}$  order parameter symmetry of  $\text{YBa}_2\text{Cu}_3\text{O}_{7-x}$  [13].

The peak structure at 89 K provides evidence that at  $T_c$  the resistance of the grain boundary bridge is much larger than the resistance of the intragrain-bridges. The observed height of the peak shown in Fig. 3 is consistent with a  $T_c$  difference of the bridges of 150 mK. The shape of the peak is influenced by the differences in the fluctuations of the intragrain bridges and the one containing the tunnel junction. Unfortunately we cannot extract data on this effect from the peak, as the spatial distribution of  $T_c$  is unknown.

The grain boundary resistance values above and below  $T_c$  extrapolate to the same value at the transition temperature. The transition into the superconducting state is therefore found not to affect the dissipation in the junctions at  $T_c$ . This observation cannot be reconciled with the predictions for surface charging effects in the hole superconductivity scenario introduced by Hirsch and coworkers [14]. In this scenario, charges are separated in the superconducting state in the vicinity of a grain boundary, but not above  $T_c$ . This charge separation is expected to change the electronic properties of the interfaces when passing through  $T_c$  [15]. The grain boundary data do not show this effect.

For  $T > T_c$ , the grain boundary resistance decreases linearly. This behavior cannot be explained by elastic tunneling from the vicinity of a well-defined Fermi surface across standard Schottky contacts with  $T$ -independent barrier heights and widths [16]. There, a

nonlinear and weak  $R_{gb}(T)$  characteristic is expected for the parameter range derived above. A more detailed elastic tunneling model has to include  $T$  dependent Schottky barriers and to consider the spatial inhomogeneity of the interface. To significantly alter the weak and nonlinear  $T$  dependence both effects demand the thermal energy  $k_B T$  to exceed the energy scales of the barrier for large parts of the interface areas. Hereby a very special energy profile of the barriers is required to yield the linear  $R_{gb}(T)$  behavior over a large temperature range. This situation seems unphysical to us. We note that inelastic tunneling via resonant impurity channels [17] cannot account for the linear temperature characteristic either. Considering the problems which standard semiconductor models have in describing the observed interface characteristics, we now turn our attention to the effect of the electronic correlations present in the cuprates.

As pointed out by Miller and Freericks [18] electronic correlations strongly affect the barrier properties of high- $T_c$  interfaces in the superconducting state. This is also true in the normal conducting state. As suggested by the band bending model [10], the barrier is an underdoped region, with the possible formation of antiferromagnetic fluctuations or even of local magnetic moments. The resultant magnetic scattering is expected to increase the interface resistance with decreasing temperature. Since the density of the magnetic moments is not known, the  $R_{gb}(T)$  dependence cannot be determined yet. Besides correlations in the barrier, electronic correlations in the bulk may also influence the transport through the interface. What would be expected if, due to the grain boundary charging, the  $YBa_2Cu_3O_7$  layers adjacent to the grain boundary were underdoped, characterized by a pseudo gap and, possibly, by preformed pairs? The spectral densities of the electronic excitations on both sides of the interface control the tunneling process. It is only for the 45 grain boundaries under consideration, that the nodal and antinodal directions of the pseudogap are directly coupled, and the tunneling current is most strongly reduced. As the pseudo gap diminishes for increasing temperature, the boundary conductivity is expected to increase. Here we note that the  $R_{gb}(T)$  curve is characterized by one temperature scale,  $T_0$ , the extrapolated zero-resistance intercept. In the samples investigated,  $T_0 \approx 350$  K, which corresponds to the

pseudo gap energy scale.

In summary, it is found that the resistance of 45° [001]-tilt  $\text{YBa}_2\text{Cu}_3\text{O}_7$  grain boundary junctions decreases linearly with increasing temperature for  $T > T_c$ . In the vicinity of  $T_c$  the grain boundary resistance and thus the dissipation are indistinguishable for  $T < T_c$  and  $T > T_c$ , in contradiction to predictions of the theory of hole superconductivity. The  $I(V)$  characteristics between 4.2 K and 300 K are nonlinear, suggesting a tunneling barrier with an effective height and width of 0.1 eV and 1.2 nm, respectively. The linear  $R_{gb}(T)$  dependence is proposed to be caused by correlation controlled tunneling.

The authors gratefully acknowledge helpful discussions with Y. Barash, H. Bielefeldt, M. Blamire, U. Eckern, P. J. Hirschfeld, C. Laschinger, J. Ransley, A. Rosch, D. G. Schlom, and M. Siegel. This work was supported by the DFG through the SFB 484 and by the BM BF via project 13N 6918A.



## REFERENCES

- [1] J.G .Bednorz and K .A .M uller, Z.Phys.B 64, 189 (1986).
- [2] S.W .Tozer et al., Phys. Rev. Lett. 59, 1768 (1987).
- [3] J.O renstein and A .J.M illis, Science 288, 468 (2000).
- [4] T .T in usk and B .Statt, Rep. Prog. Phys 62, 61 (1999).
- [5] H .H ilgenkam p and J.M annhart, Rev. Mod. Phys. 74, 485 (2002).
- [6] C .E .G ough et al., Nature 326, 855 (1987).
- [7] C .C .T suei and J.R .K irtley, Rev. Mod. Phys. 72, 969 (2000).
- [8] J.H .T .Ransley et al., IEEE Trans. Appl. Supercond. 13, 2886 (2003).
- [9] N .D .M athur et al., Nature 387, 266 (1997).
- [10] J.M annhart and H .H ilgenkam p, Mat. Sci. Eng. B 56, 77 (1998).
- [11] J.G .Simm ons, J. Appl. Phys. 34, 1828 (1963).
- [12] M .A .Scho eld et al., Phys. Rev. B 67, 224512 (2003).
- [13] C .R .Hu, Phys. Rev. Lett. 72, 1526 (1994).
- [14] J.E .H irsch and F .M arsiglio, Phys. Rev. B 39, 11515 (1989).
- [15] J.H irsch, Phys. Lett. A 281, 44 (2001).
- [16] E .L .W olf, Principles of Electron Tunneling Spectroscopy (Clarendon Press, Oxford, 1985).
- [17] L.I.G lazman and K .A .M atveev, Sov. Phys. JETP 67, 1276 (1988); err: 49, 659 (1989).
- [18] P .M iller and J.K .Freericks, Journ. of Phys. 13, 3187 (2001).

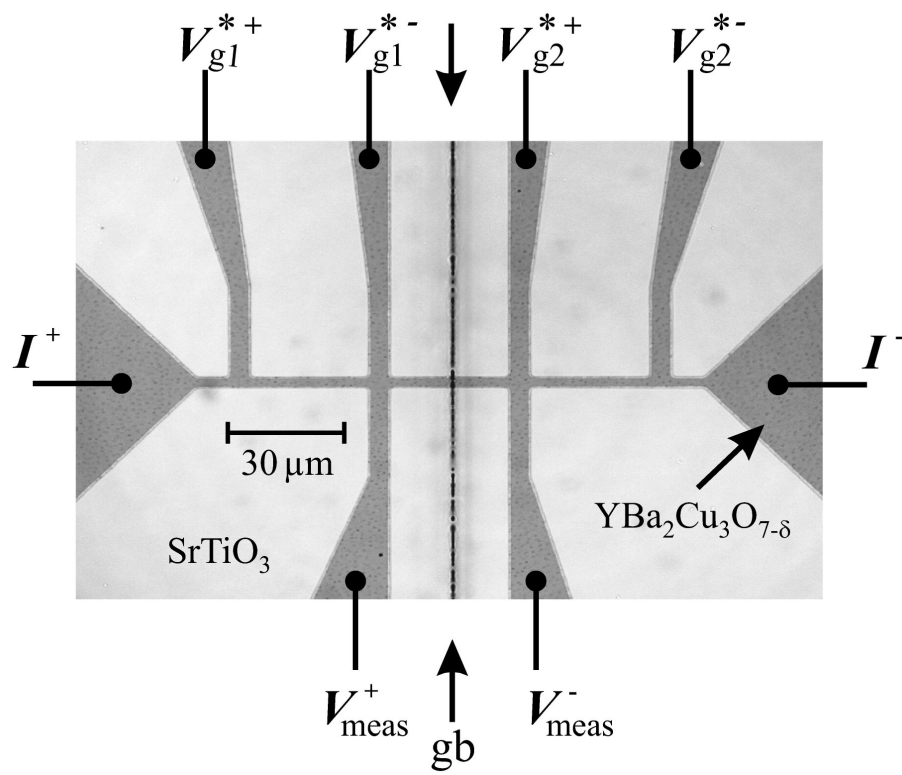
## FIGURES

FIG .1. Optical micrograph of a three-bridge sample used to measure  $R_{gb}$ . The 45° grain boundary (gb) is indicated by the arrows.

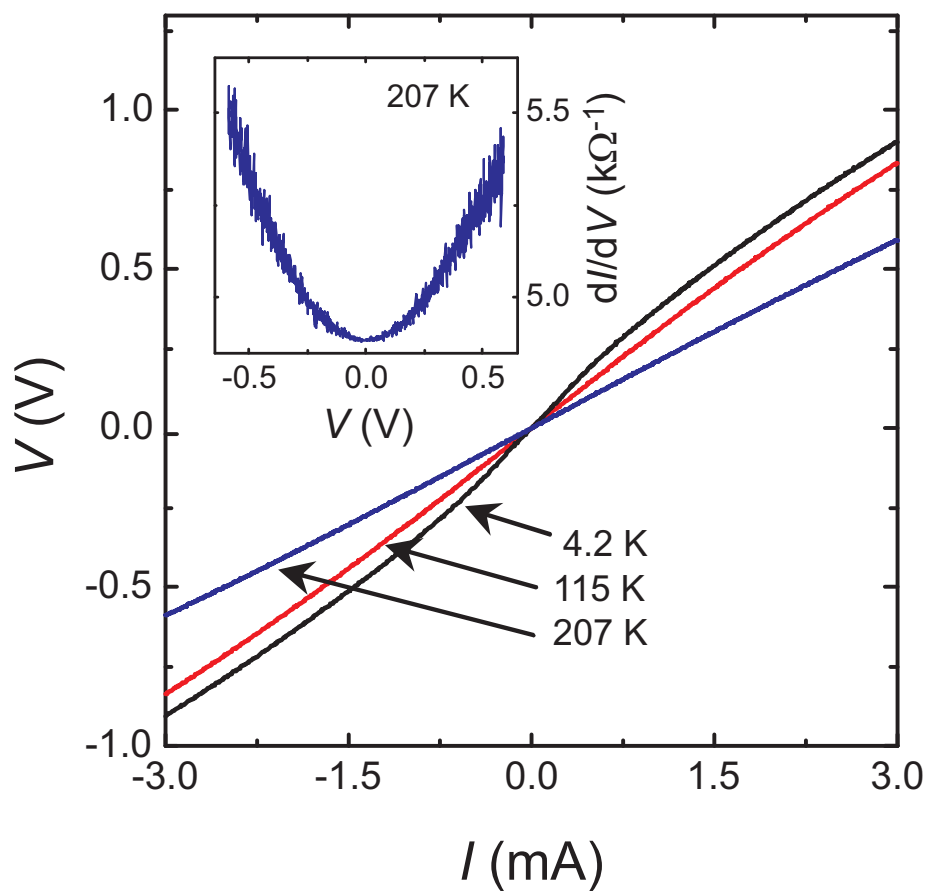
FIG .2. Current-voltage characteristics of a Wheatstone-bridge containing 23 junctions with a 45° asymmetric boundary in a 50 nm thick  $YBa_2Cu_3O_{7-x}$  film. The voltage  $V$  corresponds to the voltage across all junctions,  $V = 23 V_{gb}$ , the current  $I$  is twice the current flowing through one meander line.

FIG .3. Measured temperature dependence of the resistance of a 45° symmetric grain boundary in a 40 nm thick  $YBa_2Cu_3O_{7-x}$  film ( $I_{cr} = 100$  A). The peak reaches a maximum of 25  $\Omega$  at 88.3 K. The insets show  $dR/dT$  (T) for the grain boundary and the corresponding  $R$  (T) curve of one grain located next to the boundary.

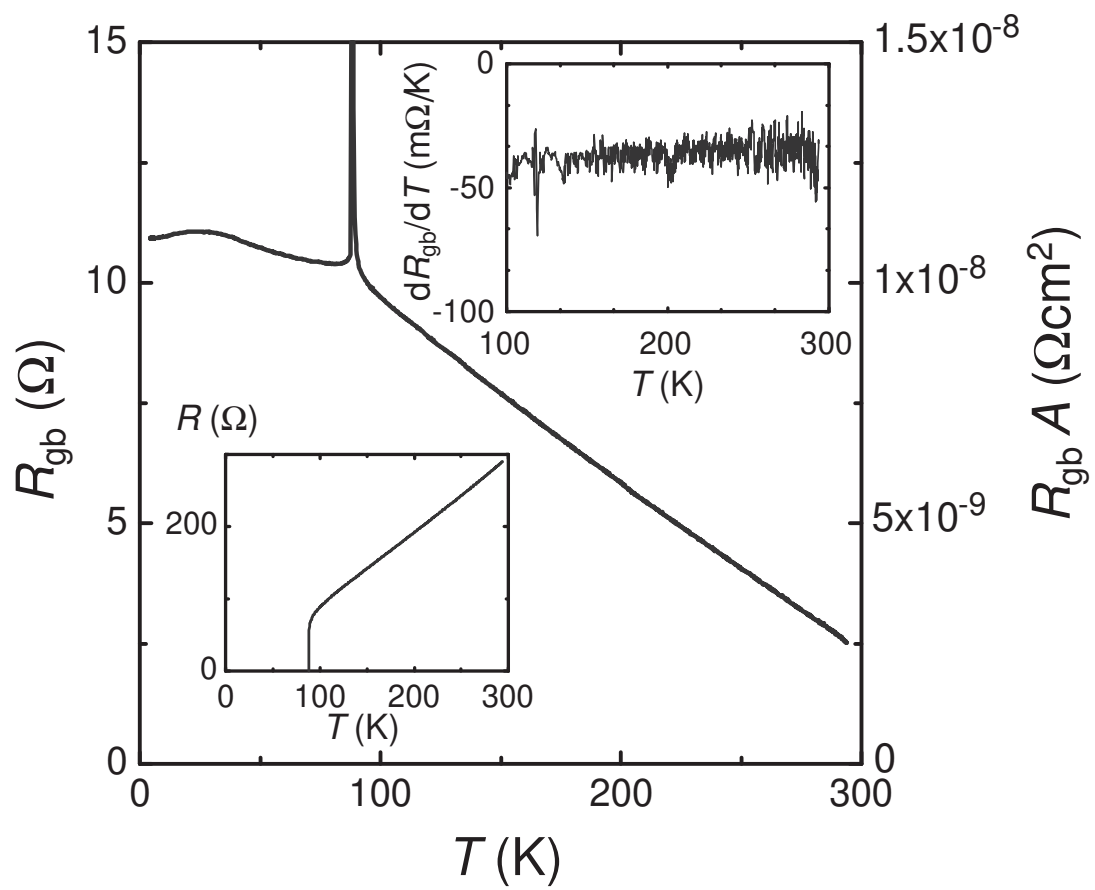
FIG .4. Temperature dependence of the resistance of a 45° symmetric grain boundary in a 40 nm thick  $YBa_2Cu_3O_{7-x}$  film measured in the three-bridge configuration. The inset shows the temperature dependent resistance of a 45° asymmetric grain boundary in a 50 nm thick film measured in a Wheatstone-bridge configuration.



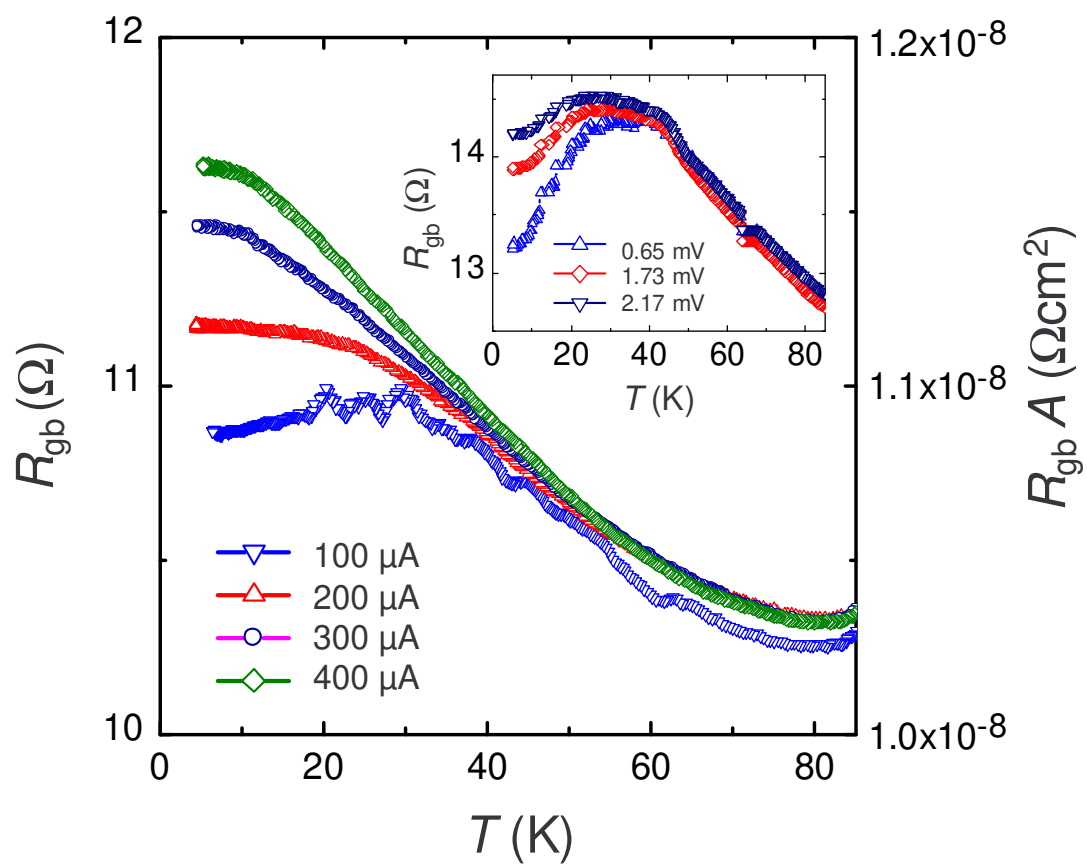
Schneider et al., Figure 1



Schneider et al., Figure 2



Schneider et al., Figure 3



Schneider et al., Figure 4